Decoupling Beam Steering and User Selection for Scaling Multi-User 60 GHz WLANs

Yasaman Ghasempour and Edward W. Knightly
Rice University, Houston, Texas, USA
{ghasempour,knightly}@rice.edu

ABSTRACT

Multi-user transmission at 60 GHz promises to increase the throughput of next generation WLANs via both analog and digital beamforming. To maximize capacity, analog beams need to be jointly configured with user selection and digital weights; however, joint maximization requires prohibitively large training and feedback overhead. In this paper, we scale multi-user 60 GHz WLAN throughput via design of a low-complexity structure for decoupling beam steering and user selection such that analog beam training precedes user selection. We introduce a two-class framework comprising *(i)* single shot selection of users by minimizing overlap of their idealized beam patterns obtained from analog training and *(ii)* interference-aware incremental addition of users via sequential training to better predict inter-user interference. We implement a programmable testbed using software defined radios and commercial 60 GHz transceivers and conduct over-the-air measurements to collect channel traces for different indoor WLAN deployments. Using trace based emulations and high resolution 60 GHz channel models, we show that our decoupling structure experiences less than 5% performance loss compared to maximum achievable rates via joint user-beam selection.

CCS CONCEPTS

• **Networks → Mobile networks**; *Wireless local area networks*;

KEYWORDS

MU-MIMO, 60 GHz, Beam Steering, User Selection, Digital Beamforming

1 INTRODUCTION

Together, millimeter-scale wavelength and GHz-scale bandwidth available at 60 GHz enable large antenna arrays, high directionality, and the potential to achieve high throughput. Today, the 60 GHz WLAN standard IEEE 802.11ad [6] supports rates up to 6.7 Gbps by transmitting to a single client at a time using analog beam steering which is discretized via predefined codebooks. In this paper, we target scaling 60 GHz WLAN capacity via *multi-user* transmission by creating opportunities for an Access Point (AP) to simultaneously transmit to multiple users with limited inter-user interference. In particular, we make the following contributions.

First, we consider a 60 GHz system architecture in which the AP has multiple Radio Frequency (RF) chains used to support simultaneous transmission to multiple clients. Moreover, the AP has many more antennas than RF chains such that each RF chain can be precoded at baseband and independently steer beams at radio frequency, often termed digital beamforming and analog beam steering respectively. We show how the achievable rate for a multi-user transmission is impacted by the selected users, analog beam steering parameters, and digital pre-coding weights, and consequently, we formulate their joint optimization. However, since the optimal solution cannot be realized in practice, we propose *decoupling* user selection and beam steering training as a simpler and lower overhead protocol structure. In this structure, each client undergoes beam steering training independent of potential grouping or multi-user transmission.

Second, we introduce a two-class framework for design and evaluation of user selection schemes in the decoupled structure. The first class, termed *Single-Shot (S^2) User Selection*, performs only based on the information obtained in beam steering training, i.e., without further measurements and in a "single shot." We design a policy in this class termed S^2 *Maximum beAm Separation* which exploits the idealized beam pattern corresponding to each user's codebook entry selected during beam training. Namely, as the name suggests, it attempts to minimize inter-user interference by selecting a group of users with minimum overlap in (idealized) beams. Here, digital training follows user selection to enable zero-forcing to mitigate residual interference. The second class, termed *Interference-aware Incremental (I^2) User Selection*, performs user selection and digital training via several rounds, with users added incrementally after AP acquisition of empirical interference information at each round. We design two policies in the class: the first adopts the same beam separation strategy as above, but also has an interference test before addition of each user; the second employs a "partitioned multi-test" in which users are partitioned according to ranked beam training information, and users in the same partition compete to be part of the selected user group. While the S^2 class is inherently simpler and lower-overhead, I^2 strategies can potentially achieve higher rates due to the additional interference information they acquire.

Third, we implement a testbed using a steerable 60 GHz RF-fronted combined with the software-defined radio platform WARP for experimental evaluation in a typical conference room. The testbed utilizes mechanically steerable horn antennas to emulate 802.11ad phased-array, and can be configured with antennas with different beamwidths. We develop a simulator that implements the key components of beam steering, digital beamforming, user selection and 60 GHz propagation characteristics using high resolution

Mobihoc '17, July 10-14, 2017, Chennai, India

ACM ISBN 978-1-4503-4912-3/17/07…$15.00
https://doi.org/http://dx.doi.org/10.1145/3084041.3084050

statistical spatial and temporal channel models developed in the literature [10, 13, 14, 17]. Moreover, for comparison purposes, we define two benchmarking algorithms which use exhaustive search to characterize the maximum achievable rate with joint user-beam selection and the decoupling structure.

Finally, we perform an extensive measurement and simulation study. We begin with a baseline case of two simultaneous users and find that two receivers cannot share an analog beam (i.e., codebook entry), even if digital precoding attempts to remove inter-client interference. Surprisingly, in such cases, zero forcing yields lower empirical sum capacity than no digital precoding. Nonetheless, we show that reducing beamwidth via a larger number of antennas not only helps prevent users from sharing the same beam, but also boosts the relative gain of zero forcing for residual interference cancellation via improved SINR. Next, we explore scaling AP's number of RF chains and streams. We show that while the performance of I^2 is able to increase with the number of RF chains (as does exhaustive search), S^2 performance *degrades* when too many streams cause excessive inter user interference that cannot be countered via zero forcing. Further, we study the case that a Line-Of-Sight (LOS) path is not available and a reflected Non-LOS (NLOS) path is required. We find that while the lower SNR inherent to NLOS users makes them less tolerant to interference, up to 12 spatial streams can be multiplexed for NLOS, LOS, and any mix of the two. Finally, we use exhaustive search to compare the decoupled structure with joint optimization. We find that despite its improved simplicity and lower complexity, decoupling beam steering and user selection incurs less than 5% capacity loss with four RF chains at the AP.

The remainder of this paper is organized as follows: Section 2 provides our multi-user architecture and explains the joint and decoupled structures for user selection and beam steering. Section 3 describes S^2 and I^2 platforms for decoupled user selection. Section 4 presents our implementation setup and benchmarks. Section 5 investigates the spatial multiplexing gains of analog/digital beamforming. Section 6 evaluates S^2 and I^2 frameworks and compares joint and decoupled structures. Finally, we discuss related work in Section 7 and conclude the paper in Section 8.

2 MULTI-USER ARCHITECTURE AND PROTOCOLS

In this section, we first describe the system architecture required to support multi-stream transmission. Next, we present the protocol and capacity implications of a decoupled vs. joint beam steering and user selection methodology.

2.1 System Architecture

60 GHz WLANs employ analog or RF beamforming to improve signal-to-noise ratio (SNR) [7, 15]. We interchangeably use the terms beam steering, RF beamforming, and analog beamforming to refer to application of different phase delays to different antenna elements in the RF domain. The IEEE 802.11ad standard supports such beam steering, but limits the AP to transmit to a single user at a time [6]. Consequently, both the AP and client require only a single RF chain for digital baseband processing. In contrast, the next 60 GHz WLAN standard IEEE 802.11ay, will supporting concurrent spatial streams from the AP to multiple clients. This requires

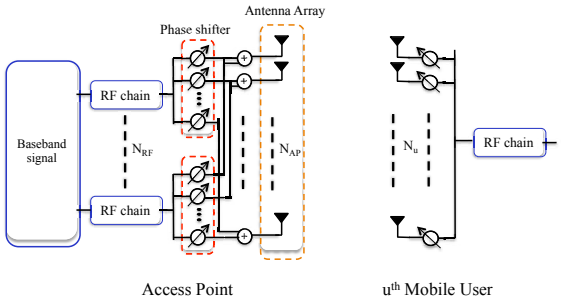

Figure 1: Hybrid beamforming architecture of AP and users.

multiple RF chains at the AP (at least one per stream) whereas the clients require only a single RF chain. Moreover, the AP's plurality of RF chains can also be used for digital pre-coding at baseband to compliment analog beam steering. Precoding schemes such as zero-forcing can be exploited to minimize or ideally cancel the inter-user interference of a multi-user simultaneous transmission [4].

Fig. 1 depicts an architecture to support such a multi-stream transmission, termed hybrid beamforming in [1, 9]. As shown, the AP (left) is equipped with N_{RF} RF chains, each capable of transmitting an independent data stream to a different client, and each can be precoded as described above. After modulation (not shown), the data streams can be independently steered with the depicted phase shifters, and the resulting signal is mapped to an array of N_{AP} antennas. The AP can simultaneously transmit to N_{RF} out of U backlogged users, with the u^{th} mobile user (right) equipped with N_u antennas. Users have only one RF chain to allow for a lower cost and more energy efficient design compared to the AP, and therefore each user can receive only one spatial stream at a time.

2.2 Achievable Multi-User Rate

The achievable sum-rate is the key metric to evaluate user selection schemes as it can incorporate gains from analog beam steering and digital zero forcing as well as detrimental effects of residual inter-user interference.

Let $w_{u,tx} \in \mathbb{C}^{N_{AP}\times 1}$ be the transmit RF beamforming vector at the AP corresponding to u^{th} user, and $w_{u,rx} \in \mathbb{C}^{N_u\times 1}$ be the receive RF combining vector at u^{th} user. Assume that the AP intends to serve users in the group G simultaneously. Further let $F_{BB} = [f_n^{BB}]_{n\in G}$ be the $|G| \times |G|$ digital baseband procoder. Then, the received signal for user $u \in G$ after hybrid analog/digital beamforming can be written as

$$y_u = w_{u,rx}^{*} \sum_{n\in G} (H_u F_{RF} f_n^{BB} s_n + n_u), \tag{1}$$

where $F_{RF} = [w_{n,tx}]_{n\in G}$, $n_u \sim N(0,\sigma^2 I)$ is the Gaussian noise, and s_n is the transmitted symbol for n^{th} user. In Eq. (1), H_u is the $N_u \times N_{AP}$ dimensional channel between the AP, transmitting with N_{AP} antennas, and user u.

Given the received signal in Eq. (1), the achievable sum-rate of the downlink simultaneous transmission to user group G, denoted

as $R_{sum}(G)$, can be formulated as

$$R_{sum}(G) = \sum_{u \in G} log_2\left(\frac{\sigma^2 + \frac{P}{|G|} \sum\limits_{n \in G} |w_{u,rx}^* H_u F_{RF} f_n^{BB}|^2}{\sigma^2 + \frac{P}{|G|} \sum\limits_{n \in G, n \neq u} |w_{u,rx}^* H_u F_{RF} f_n^{BB}|^2}\right), \tag{2}$$

where P is the fixed transmit power of the AP and $|G|$ is the cardinality of user set G.

We therefore incorporate beam steering via the F_{RF} and $w_{u,rx}$ terms and zero-forcing via the f_n^{BB} term, as they impact sum-rate of multi-user transmission to user group G. Consequently, a user grouping protocol can be viewed as targeting to select users and their transmission parameters to maximize sum-rate with minimum training and grouping overhead.

2.3 Joint User and Beam Selection: the Optimal Approach

In general, the sum-rate above can be maximized by finding the optimal subset of users ($G^\star$), optimal analog (RF) transmit beams ($F_{RF}^\star$), RF receive beams $\{w_{u,rx}^\star\}_{u \in G}$, and optimal digital (baseband) precoders ($F_{BB}^\star$) that solve

$$\begin{aligned} \{G^\star, F_{RF}^\star, \{w_{u,rx}^\star\}_{u \in G}, F_{BB}^\star\} = \arg\max & \sum_{u=1}^{U} R_u(G, F_{RF}, w_{u,rx}, F_{BB}) \\ \text{s.t.} \quad & [F_{RF}]_{:,u} \in F, u = 1, 2, \ldots, U, \\ & w_{u,rx} \in W, u = 1, 2, \ldots, U, \\ & |G| \leq N_{RF}, \end{aligned} \tag{3}$$

where the first two constraints ensure that RF beamforming and combining vectors need to be selected from the codebook F and W, respectively. RF phase shifters can only take quantized angles; hence, the analog beamforming/combining vectors can only take certain values which are stored in the finite-size pre-defined RF codebooks. The third constraint guarantees that the number of selected users is not greater than the number of AP's RF chains.

The solution to the problem in (3) requires the user set to be jointly selected with RF beamfoming/combining vectors which yields a search over the entire $\sum_{m=1}^{N_{RF}} \binom{U}{m}(F^m \times W^m)$ space of all possible user and beam combinations. Furthermore, the digital precoder F_{BB} needs to be jointly designed with the analog beamforming/combining vectors. In practice, this needs the feedback of the channel matrices H_u, $u = 1, 2, \ldots, U$. Hence, the direct solution of this sum-rate maximization requires prohibitively large training and feedback overhead. Nonetheless, we use exhaustive search in simple scenarios as a performance benchmark (cf. Section 4.3).

2.4 Decoupled User and Beam Selection

Instead of joint selection of users and beamforming weights, we employ a low-complexity structure for decoupling beam steering and user selection. The key technique is to first find analog beam steering parameters between the AP and each client, independent of potential grouping or multi-user transmission. Consequently, we term such training *Single-User Training (SUT)* since RF vectors are chosen based on the individual AP to client channels. In general, RF beamforming/combining vectors can be found by solving the following optimization problem

$$\{w_{u,tx}^\star, w_{u,rx}^\star\} = \underset{\substack{\forall w_{u,tx} \in F \\ \forall w_{u,rx} \in W}}{\arg\max} \left\| w_{u,rx}^* H_u w_{u,tx} \right\|. \tag{4}$$

The knowledge of $w_{u,tx}^\star$ and $w_{u,rx}^\star$ is sufficient to establish a directional link between the AP and user u. The complexity cost of solving Eq. (4) is $O(N^2)$, where N is the codebook size; even suboptimal standardized beam training algorithms, e.g. beamforming training in 802.11ad, require complexity of $O(N)$ [6]. The large overhead associated with RF beamforming makes it undesirable to repeat for every multi-user transmission unless the selected RF beams are not reliable anymore due to channel variations. Therefore, we decouple RF beam steering and user selection and perform the latter for each AP transmission and the former only as required.

By decoupling beam steering training from multi-user considerations, we simplify the problem in (3) to a user selection problem. Finding the digital weights is not a major challenge in the decoupled methodology since for a given selected user group and their beam steering vectors, the AP can obtain the digital beamforming weights (i.e. F_{BB}) by feeding back pilot measurements for a single user at a time, much as in conventional multi-user systems below 6 GHz. The optimal method of computing digital weights involves a technique known as Dirty Paper Coding which is difficult to implement due to high computational complexity. Instead, we utilize Zero-Forcing Beamforming (ZFBF) which is a sub-optimal yet simple method of computing digital weights.

3 A FRAMEWORK FOR DECOUPLING USER SELECTION AND BEAM STEERING

3.1 Overview

We define two complimentary classes for user selection: Single-Shot (S^2) and Interference-aware Incremental (I^2) User Selection. Both procedures employ the decoupled methodology, i.e., they first perform SUT to discover the RF beamforming/combining weights.

(i) Single-Shot (S^2) User Selection. This class of user selection schemes groups users solely based on information acquired in SUT. We name this class single-shot since user selection is performed in one epoch without further channel sounding or feedback exchange. The rationale is that the sparse-scattering nature of 60 GHz channels makes it possible to mitigate inter-user interference solely via beam steering. Thus, by utilizing the reports from SUT, single-shot schemes choose users with the lowest beam overlap and rely on ZFBF to cancel residual inter-user interference.

(ii) Interference-aware Incremental (I^2) User Selection. This class selects users via a multi-round procedure in which each round includes AP acquisition of empirical interference information and the achievable sum-rate *after* ZFBF for users included in the round. In contrast to S^2, I^2 employs incremental user selection in which users are added one by one in each round. The AP tests and trains one or more users per round, and incorporates the net positive effect of adding a user with the determinant of additional inter-user interference. While I^2 user selection can potentially achieve higher sum-rate due to additional multi-user interference measurements, it requires larger overhead compared to S^2 approaches.

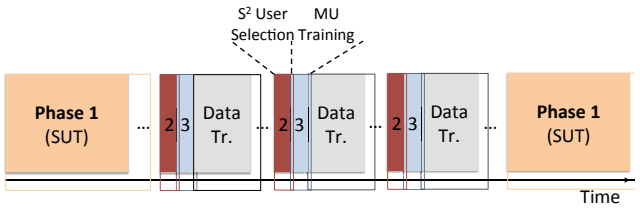

Figure 2: Single-Shot (S^2) User Selection in the context of analog and digital beamforming.

3.2 Single-Shot (S^2) User Selection

3.2.1 Overview. User selection and training procedures that are members of the S^2 can be characterized by the timeline depicted in Fig. 2. The figure shows that the Single-User Training (Phase 1) is performed initially or as needed according to client or environmental mobility, but typically at a slower time scale than packet transmission. When the AP has packets queued for multiple clients and can operate a multi-user transmission, it performs user selection using channel information only from the prior Single-User Training. The selected users can then be digitally trained for ZFBF. In particular, the three phases are as follows

SUT (Phase 1). The beam training procedure in 802.11ad consists two steps [6]. First, the AP transmits beam training frames and sweeps through all beam patterns of codebook F while the receiver adopts a quasi-omni pattern. This results in selecting the transmit RF beamforming vector which provides highest signal strength at the user, i.e., $w_{u,tx}$ for user u. Then, the user sweeps through beam patterns of codebook W while the AP is in quasi-omni mode in order to find the RF combining vector ($w_{u,rx}$). Finally, the AP and trained user exchange a feedback frame to finalize the selected beams. The AP and user adopt their selected RF vectors for this transmission. Hence, the directional single-user channel can be extracted from this feedback as

$$h_u^{SU} = w_{u,rx}^* H_u w_{u,tx}, \quad u = 1, 2, ..., U. \tag{5}$$

User Selection (Phase 2). In this class, user selection needs to be completed before digital precoding since digital beamforming weights are computed for a specific set of users to cancel or mitigate their inter-user interference. Therefore, user selection is the intermediate step between the analog and digital precoding as depicted in Fig. 2. Available information for S^2 user selection includes not only the above Phase 1 information, but also the AP system state. Namely, the AP knows the hardware configuration of itself and its users such as the number of transmit antennas (N_{AP}), number of RF chains (N_{RF}), the number of users (U), and the finite-size RF codebooks (W and F).

Thus, we define the family of S^2 user selection to include all schemes that rely on the above information

$$\mathcal{G} = f(N_{RF}, U, N_{AP}, W, F, \{w_{u,tx}\}_{u=1}^{U}, \{h_u^{SU}\}_{u=1}^{U}), \tag{6}$$

where $\mathcal{G}$ is the set of users that are co-scheduled (grouped). In Eq. (6), N_{RF}, U, N_{AP}, W, F are system state information, $\{w_{u,tx}\}_{u=1}^{U}$ and $\{h_u^{SU}\}_{u=1}^{U}$ are beam training information. Thus, a user selection mechanism that does not require any extra information is a member of this class.

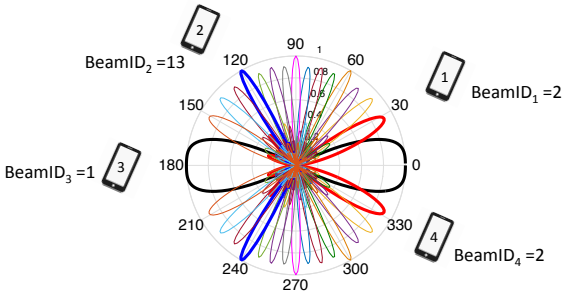

Figure 3: Illustrative scenario for S^2-MAS: one AP with 16 beam patterns and four users.

Multi-user Zero-Forcing (Phase 3). In order to cancel the residual inter-user interference of the co-scheduled (selected) users, the AP can exploit common digital precoding schemes (e.g., ZFBF). Thus far, the AP knows selected user group $\mathcal{G}$ and RF beamforming vectors from Phase 1 and Phase 2. Therefore, the directional channel between the AP and user group $\mathcal{G}$ can be measured as follows

$$\begin{aligned} \bar{h}_u &= w_{u,rx}^* H_u [w_{u,tx}]_{u\in\mathcal{G}}. \\ \bar{H}_{\mathcal{G}} &= [\bar{h}_u]_{u\in\mathcal{G}}. \end{aligned} \tag{7}$$

Applying ZFBF scheme, the digital weights (i.e., $F_{BB}(\mathcal{G})$) will be

$$F_{BB}(\mathcal{G}) = \bar{H}_{\mathcal{G}}^*(\bar{H}_{\mathcal{G}}\bar{H}_{\mathcal{G}}^*)^{-1}. \tag{8}$$

Once user selection and digital training are complete, the AP is ready to transmit independent streams to users in $\mathcal{G}$ simultaneously.

3.2.2 S^2 Maximum beAm Separation (S^2-MAS). We define an exemplary single-shot user selection strategy which groups users based on the selected beams, targeting maximum beam separation. The relative beam separation of two users can be realized via their RF beamforming vectors selected in SUT. In particular, we define $BeamID_u$ associated with user u as the index of its RF beamforming vector (i.e, $w_{u,tx}$) among columns of AP's codebook. We elaborate on $BeamID_u$ and illustrate S^2-MAS strategy via an example.

Fig. 3 depicts an example scenario in which the AP generates 16 beam patterns with 16 antenna elements based on the codebook proposed in [8]. Four users and their associated beam IDs are shown in this picture. Every beam pattern has two strong main lobes and multiple side lobes. For illustration, assume we intend to group an additional user with User 1 via S^2-MAS selection policy for a two-user simultaneous transmission. As shown in Fig. 3, the second beam pattern (red) is the directional beam that corresponds to User 1 (i.e. BeamID$_1$ = 2). S^2-MAS selects User 2 with BeamID$_2$ = 13 to be grouped with User 1 since it has the maximum Beam ID distance with User 1 compared to others. As we observe, the outcome of this selection policy depends on the beam patterns (or RF codebook) at the AP and not the physical angular distance between users; for instance, User 3 has the highest angular separation with User 1 ($\sim 120°$) but small Beam ID distance and is not selected via S^2-MAS. Note that after the user selection phase, the AP and users will undergo digital training to best cancel out any residual inter-user interference as described above.

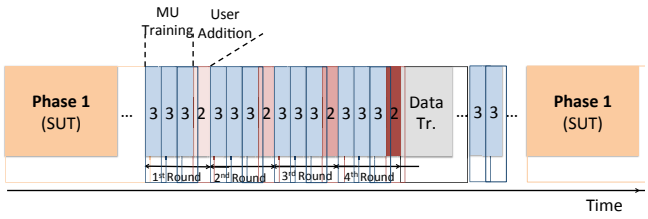

Figure 4: Interference-aware Incremental (I^2) User Selection in the context of analog and digital beamforming.

3.3 Interference-aware Incremental (I^2) User Selection

3.3.1 Overview. I^2 user selection employs interference-aware user addition with a measurement and feedback round for addition of each user. Namely, I^2 adopts a multi-round procedure for testing and training each additional user, incorporating the net positive effect of adding a new user with the detriment of additional inter-user interference.

Fig. 4 depicts the I^2 mechanism in which SUT is completed as the first phase similar to single-shot procedure. Subsequently, user selection and digital training are performed via several rounds (e.g., Fig. 4 shows four rounds). In each round, the AP acquires empirical interference information of one or many candidate users (in Fig. 4, three potential users are assumed in each round). Hence, the AP estimates the achievable sum-rate when a potential user is grouped with already selected users. Let G_{i-1} be the user group at the end of $(i-1)^{th}$ round and n be the index of the user which provides the highest sum-rate among potential users in round i. If the collected interference information shows that $R_{sum}(G_{i-1} \cup \{n\}) > R_{sum}(G_{i-1})$, the AP proceeds to the next iteration and adds user n to the group (i.e., $G_i = G_{i-1} \cup \{n\}$). Otherwise, the user addition is terminated and the AP transmits to user group G_{i-1}. While incremental algorithms potentially provide higher data rates due to measurement-based interference-aware addition of users, complexity and overhead time for feedback is increased compared to single shot.

3.3.2 Example User Selection Policies. Here, we define two exemplary strategies.

(i) I^2 Maximum beAm Separation (I^2-MAS). We define I^2-MAS as an incremental user selection strategy, in which an additional user is added in each round as follows. Like S^2-MAS, I^2-MAS targets adding user which has maximum beam. In contrast, I^2-MAS adds users one by one and not all in one-shot. This enables the AP to evaluate the achievable sum-rate of multi-user transmission as the user group grows. User selection is terminated when adding one more user decreases the achievable sum-rate due to excessive inter-user interference or serving another user is impossible due to lack of RF chains. At this stage, ZFBF training has already been performed for all users in the group and transmission can occur.

(ii) I^2 Partitioned Multi-test (I^2-PM). We define I^2-PM as an incremental algorithm, in which for each round, multiple users are tested/trained and the one that maximizes the sum-rate will be added to the existing group. The algorithm first sorts users in descending order according to the norm of their single-user channels (i.e., h_u^{SU} for user u which is available after SUT and formulated in Eq. 5). Then, I^2-PM partitions users into N_{RF} partitions and labels them from 1 to N_{RF} such that partition 1 includes $\lceil U/N_{RF} \rceil$ users with the highest channel norms, partition 2 with the second highest, etc. For any pre-selected first user, the algorithm finds the partition index which contains this user (denote this index as i). I^2-PM tests all users in the $(i+1)^{\text{th}}$ partition by measuring their channel state information to calculate their induced interference and their achievable sum-rate when grouped with already selected user(s). Next, the user from the partition with the maximum sum-rate is selected and the algorithm proceeds by updating $i \equiv i+1 \pmod{N_{RF}}$ and continuing the same procedure. This incremental addition can happen at most $N_{RF}-1$ times and, like I^2-MAS, user addition terminates when the sum-rate would degrade even for the best tested user. While I^2-PM tests multiple users in each round, the test only involves $\lceil U/N_{RF} \rceil$ users belonging to one partition, thus reducing complexity compared to exhaustive testing of all users in each round. Therefore, the total number of tests for I^2-PM is $O(U)$ vs. $O(U \times N_{RF})$.

4 EVALUATION SETUP: TESTBED, TRACE DRIVEN EMULATION, AND BENCHMARKS

In this section, we describe our testbed implementation, trace-driven emulation, and introduce two algorithmic benchmarks.

4.1 Testbed Implementation

We use the testbed setup from [12] enhanced as follows: our testbed consists of commercial mm-wave transceivers from the VubIQ 60 GHz development system, two WARP v1 boards, and circuits for signal adjustment outlined in Fig. 5a. The mm-wave transceivers are capable of communicating in 57-64 unlicensed band with up to 1.8 GHZ modulation bandwidth. Using WARP-lab [11] and VubIQ control panels, we apply the transmit module as the AP and the receive module as the client. Random binary data is generated via WARPLab and encoded using BPSK. The VubIQ module converts the signal to 60 GHz band and horn antennas provide directional transmission emulating phased array antennas. To achieve different beamwidths, we configure 7°, 20° and 80° horn antennas. In the receiver's VubIQ module, the signal is received by a horn antenna and is downconverted to analog I/Q baseband. In order to collect Received Signal Strength (RSS) for different locations and antenna orientations, we use mechanical motors and DC microstep driver with a motion control setup connected to the transceivers to steer the beams with sub-degree accuracy.

4.2 Trace-Driven Emulation

With the 60 GHz testbed, we can measure RSS of a point to point transmission but not multi-user concurrent transmission since each WARP board is equipped with a single RF chain. While analog beamforming is possible with the help of mechanical motors which allows the transmitter to steer, digital beamforming requires the transmitter to obtain channel information to construct digital weights.

In order to obtain this channel matrix, we adopt the high resolution millimeter wave channel models from the literature [10, 13, 14, 17]. These channel models are designed based on measurement campaigns in different LOS and NLOS environments. We can compute the channel matrix (H) between any two nodes via these

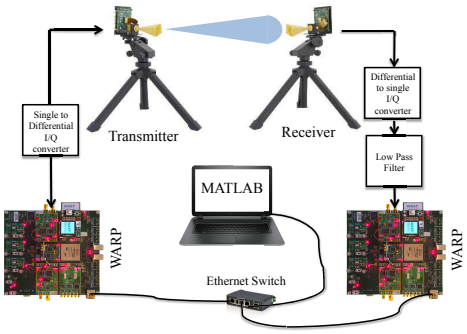

(a)

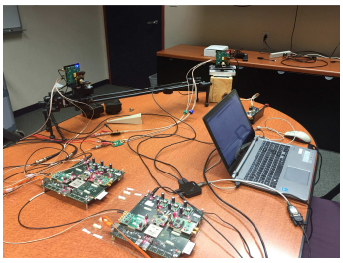

(b)

Figure 5: (a) 60 GHZ hardware blocks. (b) The 60 GHz setup in a conference room where the data was collected.

channel models and compute the analog beamforming or digital weights. To confirm the integrity of the obtained channel matrix, we use our 60 GHz testbed to measure the main components of the channels such as RSS, Angle of Departure (AoD) and Angle of Arrival (AoA) of the LOS path and strong reflected paths in a similar scenario (i.e, same distance and orientation). We perform over 10,000 measurements varying receiver location, antenna orientation, and RF beamwidth, and all data sets will be available online upon publication. We observe an average error of 7.02% in RSS values by directly comparing measurements and simulations. We present results using simulations that incorporate measurement data for parameter setting as well as channel traces as feasible.

4.3 Benchmarking Algorithms

For evaluation purposes, we introduce two benchmarking algorithms for joint and decoupled user and beam selection.

(i) Exhaustive decoupled. In this algorithm, we adopt Single-User Training to find the RF beamforming/combining vectors corresponding to each user. However, for user selection, the algorithm goes over $\sum_{m=1}^{N_{RF}} \binom{U}{m}$ possible user combinations. For a test user group G_t, it computes zero-forcing weights based on Eq. (8) and then calculates $R_{sum}(G_t)$ according to Eq. (2). The algorithm records the achievable rate of all possible user groups and picks the one with maximum sum-rate. Note that *Exhaustive decoupled* provides an upper-bound for the achievable sum-rate via decoupling beam steering and user selection.

(ii) Exhaustive joint. We formulated the general problem of user selection, RF beamforming and digital precoding in (3). The optimal solution of (3) given a fixed digital precoding scheme (e.g., zero-forcing) yields to an exhaustive search over all possible user-beam tuples. We call this algorithm *Exhaustive joint* since it searches through all different (user, beam) combinations. The search space includes $\sum_{m=1}^{N_{RF}} \binom{U}{m}(F^m \times W^m)$ distinct combinations where F and W are AP's and users' codebooks, respectively. Implementation of *Exhaustive joint* algorithm may not be practical in real scenarios due to the high computational complexity; however, comparing it with *Exhaustive decoupled* algorithm determines the performance loss due to decoupling beam steering and user selection. We quantify and analyze this performance loss in Section 6.4.

5 RECEIVER SEPARATION AND ARRAY SIZE

In this section, we experimentally characterize the spatial multiplexing gains of beam steering with and without ZFBF for indoor WLANs. We consider two receivers and investigate empirical capacity as a function of receiver separation as well as array size.

5.1 Receiver Separation

Below 6 GHz, multi-user transmission with spatial multiplexing was demonstrated to be achievable even with sub-wavelength receiver separation [3]. However, [3] exploits increased multi-path than is available at 60 GHz and employs one RF chain per *antenna*. Here we explore the required receiver separation for the case of only one RF chain per *user*.

Scenario. We designed a scenario depicted in Fig. 6a consisting of an AP with two RF chains simultaneously transmitting to two receivers. The first receiver, R_1, is at a fixed location, whereas the second receiver, R_2, is placed at 12 different locations as labeled in Fig. 6a . In these experiments, the AP always has LOS components to both receivers. We perform Single-User Training (SUT) using the beam patterns in Fig. 3 and find the empirical capacity of single-user transmission to R_1. This empirical capacity is computed based on the RSS at R_1 using beams chosen in SUT. We validated the RSS of single-user transmission to R_1 and R_2 (in all 12 locations) through measurements using 20° horn antenna at the transmitter. For each of the location IDs in Fig. 6a, we perform simultaneous transmission to R_1 and R_2 via beam steering with and without ZFBF. In beam steering only, we skip the the digital training and only apply RF beamforming/combining vectors found via SUT. When turning on ZFBF, the two RF chains are pre-coded with weights computed based on Eq. (8). Although measuring channel matrix and zero-forcing weights is not possible due to hardware limitations, we validated the main components of channels such as RSS, AoA and AoD of the LOS path.

Fig. 6b depicts the capacity gain of two-user simultaneous transmission over single-user transmission to only R_1 for the different locations of R_2. As a baseline, single-user transmission to R_1 achieves 5.8 bps/Hz rate in average. First, the figure shows that when the two receivers are in the same beam as in locations 11 and 12, ZFBF cannot mitigate inter-user interference such that it is preferable to transmit to only one user than to transmit to two users when they are both within the same analog beam. Likewise, the same effect occurs for the backlobe, as location 7 with 180° angular separation also yields a capacity decrease (also cf. Fig. 3). Note that here, no strong NLOS path is available to R_1 and R_2. If they were, the AP might be able to create "separate beam" transmission via NLOS

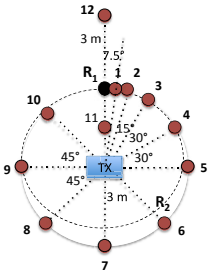

(a) Evaluation scenario

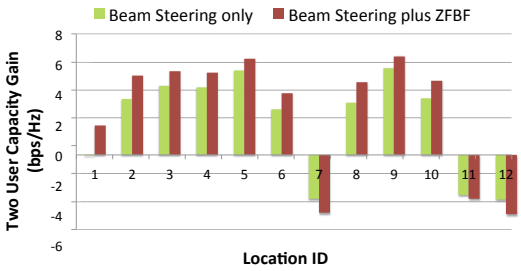

(b) Sum capacity as a function of location

Figure 6: Sum-capacity as a function of receiver separation.

path, even if users are along the same LOS path, and still obtain positive capacity gain from multi-user transmission.

Second, in the cases in which two receivers have the same selected RF beams (locations 7, 11, and 12), employing ZFBF for multi-user transmission is *worse* than purely analog beam forming. The reason is that ZFBF is a sub-optimal precoding scheme which works best in high SINR regimes. (Optimal precoding, Dirty Paper Coding, is difficult to implement due to computational complexity.) When the selected RF beams for two receivers have sufficient overlap, the linear processing at the user will not be sufficient to overcome the high path loss plus the inter-user interference.

Here, beam patterns have half power beam width (HPBW) of 15°. Thus, the angular separation between R_2 and R_1 is greater than the $0.5 \times HPBW$ for locations $2-6$ and $8-10$ and equals to $0.5 \times HPBW$ for location 1. Third, Fig. 6b shows that when the angular separation between two receivers is greater than the $0.5 \times HPBW$, ZFBF provides an average capacity boost of 27% over beam steering without ZFBF. Indeed, the highest capacity gain belongs to locations 5 and 9 with minimum beam overlap with R_1.

Finding: Two receivers cannot share an analog beam (less than $0.5 \times HPBW$ angular separation) even when they also perform inter-user interference cancellation via zero forcing. Indeed, zero forcing was detrimental compared to no digital precoding as it was an ineffective mechanism in the low SINR (high interference) regime.

5.2 Antenna Array Scaling and Beamwidth

The width of the beam patterns generated by an analog codebook depends on the number of antenna elements with larger arrays generating higher gain with more focused beams. IEEE 802.11ad allows beams as narrow as 3° [6]. Narrow and highly directional beams not only increase received signal strength at the intended receiver(s),

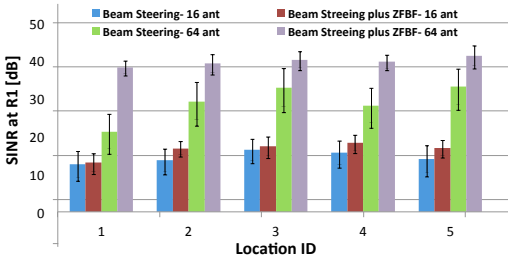

Figure 7: SINR at R_1 when grouped with R_2, which is placed in five different locations.

but may also help suppress interference at other receivers. Previously, we observed that in two-user LOS scenario with 15° HPBW, ZFBF can achieve 27% capacity boost provided that receivers are in separate beams. Here, we investigate the impact of beam width (equivalently, number of antenna elements) on the performance gain of ZFBF to mitigate the inter-user interference.

Scenario. We employ the same node deployment setup of Fig. 6a. However, instead of finding capacity gain, we study the received SINR at R_1 in a two-user transmission to directly study the impact of ZFBF on the interference reduction. The AP uses 16-element (as above) or 64-element arrays (i.e., $N_{AP} = 16$ or 64) and beam steers with and without ZFBF. The 16-element antenna array can generate beam patterns with approximately 15° HPBW while the 64-element array makes 4° beams. We repeat this experiment for different locations of R_2 (location ID 1 to 5 as depicted in Fig. 6a). In all topologies, R_1 and R_2 have LOS connectivity with the transmitter. Fig. 7 shows the SINR variation at R_1 when grouped with R_2, in which R_2 is placed in five locations (as in x-axis).

First, as expected, beam steering with 64 antenna elements provides higher antenna gain, and higher SINR consequently, compared to 16-elements. Even though R_1 is fixed, its SINR is vulnerable to change significantly depending on the location of R_2 when the AP only employs beam steering and forgoes digital training via ZFBF. Furthermore, narrower beams are more vulnerable to SINR change as the figure shows larger error for beam steering only with 64 antennas compared to the 16 antennas.

Second, Fig. 7 reveals that ZFBF provides greater SINR boost when beam steering employs a 64-element array (4° beams). Specifically, in location 1, ZFBF achieves 2× SINR gain with 64 antenna element and 1.04× gain with 16 antenna elements. On one hand, increasing the number of antenna elements at the AP reduces the inter-user interference by generating more focused beams; hence, making less opportunity for ZFBF to boost the SINR by canceling out the residual inter-user interference. On the other hand, larger antenna arrays provide higher spatial diversity which can be further exploited by ZFBF to boost SINR. The figure shows that the latter outweighs the former such that ZFBF can provide greater SINR boost, and consequently capacity boost, even if highly directional beams are adopted at the transmitter.

Finding: ZFBF can provide greater SINR boost, and consequently higher capacity gain, as the transmitter is equipped with larger antenna arrays or equivalently more directional beams in a multi-user transmission, even having the same number of RF chains.

6 EVALUATION OF DECOUPLED USER AND BEAM SELETION

In this section, we evaluate S^2 and I^2 strategies, first focusing on the LOS case and investigating the impact of scaling group-size. Subsequently, we compare the performance of user selection strategies in LOS and NLOS connectivity and study the impact of link connectivity on the spatial multiplexing. Lastly, we analyze the performance loss due to decoupling user and beam selection.

6.1 Scaling Group Size (LOS only)

We evaluate *S^2-MAS* as a single-shot user selection policy and *I^2-MAS* and *I^2-PM* as interference-aware incremental policies. For comparison purposes, we also present results for *Exhaustive decoupled* and *Random* user selection.

Scenario. We deploy ten different node setups with each having 40 users randomly placed in a 6×6 m^2 indoor environment with the AP in the center and a LOS path between the AP and each user. We equip the AP with $N_{RF} = m$ RF chains, so that it can multiplex up to m data streams to m users (m can be 2, 3, 4, and 5 in this experiment). The AP has a codebook consists of 32 beam patterns while each user is equipped with a single RF chain and 4 beams. For each configuration, we perform Single-User Training (SUT) and employ the selected RF beams for 40 sequential user groupings and data transmissions. In our setup, nodal and environmental mobility is negligible such that SUT information is reliable, even when used at a later time. We let user i be the prime (pre-selected) user in multi-user transmission i and perform *Random*, *S^2-MAS*, *I^2-MAS*, *I^2-PM* and *Exhaustive decoupled* user selection algorithms to group other user(s) with user i. In all cases, we apply ZFBF to suppress inter-user interference and find the average empirical sum-capacity of the simultaneous transmission to the selected group.

Fig. 8 depicts empirical sum-capacity averaged over all sub-topologies vs. the number of RF chains. First, the figure shows that *Random* is the only technique with decreasing sum-capacity as the number of RF chain increases. This is because *Random* aggregates as many users as RF chains, N_{RF}, without considering their mutual interference. While for 2 RF chains, random user selection often selects users in separate beams, with 3, 4, and 5 simultaneous users, this is increasingly unlikely. Moreover, despite having an increased number of RF chains to support digital beamforming, ZFBF is unable to correct for the poor user grouping, as was also the case with two RF chains in Section 5. Hence, *Random* selection achieves 61% of the maximum sum-capacity (via *Exhaustive decoupled*) with 2 RF chains, and only 16% with 5 RF chains.

Second, the S^2-MAS policy yields only a marginal improvement with an increasing number of RF chains beyond 2, and even slightly degrades sum capacity with 5 RF chains. Like *Random*, S^2-MAS always uses the maximum group size (the number RF chains at the AP) and employs ZFBF to cancel out any residual interference. Yet unlike *Random*, the S^2-MAS policy mitigates inter-user interference by selecting users according to their RF beams (and not randomly). Unfortunately, for larger groups, the interference can be excessively high: With users randomly located in the environment, there is often no user in a position which is sufficiently angularly separated from already selected users. While for 2 RF chains, this probability is low, with 3, 4, and 5, this becomes increasingly problematic such

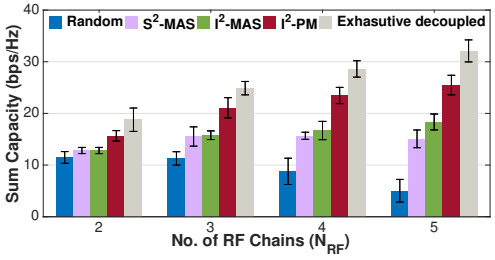

Figure 8: Achievable sum capacity with S^2 and I^2 policies under different number of AP's RF chains.

that with 5 RF chains, S^2-MAS achieves only 47% of the capacity of Exhaustive decoupled approach.

Third, Fig. 8 reveals that I^2 policies *I^2-MAS* and *I^2-PM*, never lose sum-rate due to an additional RF chain at the AP. By design, I^2 schemes add users sequentially and evaluate the net effect of adding another user before data transmission.

Finally, although the sum rate of *I^2-MAS* modestly increases with the number of RF chains, it cannot keep up with *I^2-PM*: With larger user groups, the amount of induced inter-user interference by an additional user would be higher. Thus, it is more important to test multiple users in each round to find the one that can tolerate the inter-user interference and boost the sum-rate.

Finding: While both S^2 and I^2 polices perform nearly equally well with two RF chains, the performance gap between them increases as the number of RF chains at the AP increases, with S^2 policies even having degraded performance with more RF chains due to excessive inter-user interference that ZFBF cannot mitigate.

6.2 LOS vs. NLOS Connectivity

Here we consider scenarios in which no LOS path is available due to blockage and therefore the AP must connect via a reflected path.

Scenario. We adopt the same node deployment setup except that we block the LOS path from the AP to each user. Consequently, the AP finds a reflected path (e.g., off of a table or wall) during SUT. Fig. 9 depicts the empirical capacity for an AP with 4 RF chains. In addition to the NLOS scenario, it also depicts LOS as a baseline. The figure is normalized to the capacity of *Exhaustive decoupled* for the respective scenarios. First, the figure indicates that all user selection schemes perform closer to *Exhaustive decoupled* in LOS than NLOS: In the NLOS scenario, because the received signal strength is lower, there is less residual tolerance for inter-user interference. Therefore, it is more important to apply a user selection strategy which selects users with minimum inter-user interference in such scenarios, and all policies end up far from what can be achieved by *Exhaustive decoupled* in the NLOS case.

As observed in Fig. 9, with NLOS, *S^2-MAS* and *I^2-MAS* can only achieve 23% and 30% of *Exhaustive decoupled* sum-capacity. These strategies select users according to their beam separation to mitigate interference at receivers. In NLOS case, the RF beam is mostly locked into the strongest NLOS path. In such scenarios, the high beam separation does not necessarily mean low inter-user interference. For example, in an extreme example, two users which are co-located may see two strong NLOS paths (e.g., off two walls) from the AP.

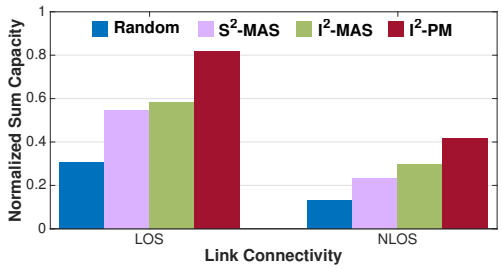

Figure 9: Normalized capacity of S^2 and I^2 policies under LOS and NLOS link connectivities with a four-RF chain AP.

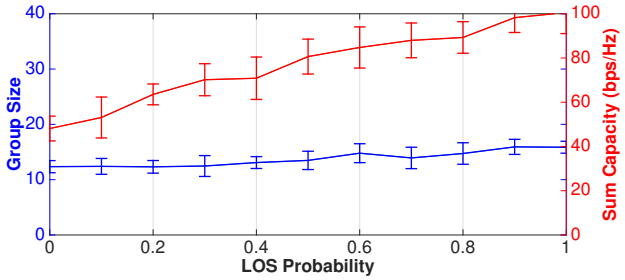

Figure 10: The sum capacity and group size of Exhaustive decoupled search as a function of LOS probability.

While in SUT, each can lock its RF beam to a different NLOS paths, both users still experience significant interference from the other NLOS path. This would not be an issue in LOS scenario since the RF beam is mostly locked to the LOS path in SUT which is significantly stronger than any NLOS path. Thus, beam separation based policies perform poorly in NLOS scenarios.

Even *I^2-PM* which provides 82% of *Exhaustive decoupled* capacity in LOS connectivity, achieves only 42% of the maximum sum-rate in NLOS. *I^2-PM* searches through a subset of users (i.e, $\lceil U/N_{RF} \rceil = 10$ users here) in each round. Considering the lower RSS of NLOS users, it becomes increasingly likely that *I^2-PM* cannot find a user (out of 10 users) which improves the sum-capacity and makes it terminate the multi-round procedure.

Finding: User grouping algorithms that select users according to RF beam separation are vulnerable to performance loss in NLOS environments in which the dominant LOS path is unavailable or blocked. NLOS users can tolerate less inter-user inference as their RSS is reduced due to lack of a LOS path.

6.3 Maximum Multiplexing Potential: Mixing LOS and NLOS

We now investigate the impact of link connectivity on the spatial multiplexing potential which is quantified via two metrics: (i) maximum achievable capacity via *Exhaustive decoupled* search; (ii) the maximum number of users that can be simultaneously served. To find the impact of link connectivity, we define a new factor termed *LOS Probability* which characterizes the fraction of users that have a LOS path to the AP.

Scenario. We deploy 10 different node setups in which 32 users are placed randomly in a $6 \times 6\, m^2$ environment. The AP is equipped with 32 RF chains and its RF codebook consists of 32 beams (i.e., $U = N_{RF} = 32$). Users have a single RF chain with four beam patterns. Therefore, the AP has a sufficient number of RF chains to serve all users concurrently. For each node deployment topology, we vary the *LOS Probability* from zero to one by blocking a subset of paths, zero indicating that all users have only NLOS paths.

Fig. 10 depicts the number of simultaneous users (group size) and the empirical sum-capacity vs. *LOS probability*. The figure reveals that even with only NLOS (LOS probability of 0), the AP is capable of serving 12 users for multi-user concurrent transmission, i.e., 13 users would have yielded lower capacity due to excessive interference. While the number of simultaneous users varies slightly with LOS probability, we observe that the empirical sum-capacity of *Exhaustive decoupled* increases roughly linearly with LOS probability. Namely, the LOS users have higher RSS and per-user data rate, so that even with the same group size, the achievable sum-rate in LOS scenario would be almost two times of the NLOS.

Finding: Even though NLOS users experience reduced SNR, 12 spatial streams can be multiplexed via Exhaustive decoupled search for LOS, NLOS and any mix of the two.

6.4 Joint User-Beam Selection vs. Decoupled

Here we evaluate the *Exhaustive joint* algorithm which provides the optimal solution to the problem of joint user and beam selection in (3) given a fixed digital precoding scheme such as zero-forcing. *Exhaustive joint* searches through all user-beam tuple combinations while *Exhaustive decoupled* performs SUT separated from user selection. Thus, we investigate the performance loss incurs by decoupling beam steering from user selection.

Scenario. We place 20 users in random locations within a $12 \times 12\ m^2$ indoor environment. The AP is equipped with $N_{AP} = 24$ antennas and $N_{AP} = 2$ RF chains while users have only one RF chain and one antenna for simplicity. We compare the achievable sum-rate for multi-user transmission via *Exhaustive decoupled* and *Exhaustive joint* algorithms and refer to them as R_d and R_j, respectively. We repeat the experiment for 3 and 4 RF chains at the AP, when all users having LOS or NLOS connectivity.

We compare the performance of these two algorithms in Table 1 in which the first column shows the scenario and the second column reports the percentage of R_d over R_j. We count the number of observations in which *Exhaustive decoupled* provides the optimal user-beam set and report this count ratio over total number of observations as $Prob(R_j = R_d)$ in the third column.

Table 1: *Exhaustive decoupled* compared to *Exhaustive joint*.

Scenario	$\frac{R_d}{R_j}\%$	Prob $(R_j = R_d)$
$N_{RF} = 2$, LOS	98.26	0.63
$N_{RF} = 2$, NLOS	98.22	0.57
$N_{RF} = 3$, LOS	98.06	0.52
$N_{RF} = 3$, NLOS	97.44	0.42
$N_{RF} = 4$, LOS	95.79	0.41
$N_{RF} = 4$, NLOS	95.19	0.37

First, we observe that *Exhaustive decoupled* achieves more than 95% of the optimal sum-rate with four simultaneous users. However, the performance loss slightly increases as the number of RF chains at the AP increases since the joint methodology is able to reduce the excessive inter-user interference by jointly configuring analog beams and users to be served. Due to computational limitations, we could not investigate scenarios with more than 4 RF chains.

Second, the table reveals that with the same number of RF chains, LOS connectivity results in higher $Prob(R_j = R_d)$ compared to NLOS. R_j differs from R_d when the set of selected user-beam tuples via *Exhaustive decoupled* does not match the outcome of *Exhaustive joint* algorithm. There are two possibilities: the *Exhaustive joint* search may choose *(i)* different users; or *(ii)* the same users but different RF beams. The LOS path (if exists) is significantly stronger than other NLOS paths such that the choice of RF beam mostly depends on the LOS path and not the partnered (grouped) users. Hence, in LOS case, the possibility of the latter case (same users with different RF beams) is lower and $Prob(R_j = R_d)$ is larger.

Finding: Decoupling beam steering and user selection results in 5% capacity loss compared to joint user-beam selection with four simultaneous users. However, the performance loss increases in the NLOS scenario and as the group size increases.

7 RELATED WORK

Multi-user Beamforming. Prior work on multi-user beamforming in millimeter-wave networks focuses on developing low-complexity algorithms that can achieve near-optimal capacity performance [1, 16]. Such work does not address user selection, and instead aims to maximize the capacity of simultaneous transmission to a given group of users by adjusting digital and analog weights. Consideration of user selection would create a dependency in which the choice of RF beamforming affects user selection, and consequently, the digital precoder to cancel out the inter-user interference of the selected users. In contrast, in this paper, we do not design new analog/digital beamforming algorithms; instead, we design and analyze user and beam selection procedures that can be applied to a broad class of beamforming algorithms.

User Selection. Extensive prior work has addressed user selection and grouping in MU-MIMO systems which operate below 6 GHz. Example results include user grouping based on channel state and/or expected transmission time [5, 18, 19]. Likewise, other work has targeted user grouping without channel state information by exploiting the rich scattering propagation environment indoors below 6 GHz [2, 20]. In contrast, we consider both a different frequency band and node architecture: 60 GHz channels lack the rich scattering properties observed below 6 GHz [10]; moreover, as described in Section 2, we consider that each RF chain has multiple antennas available to it which can be controlled via analog beam steering weights such that the SUT phase considered here does not exist in the aforementioned prior work.

8 CONCLUSION

We introduced and evaluated two structures, S^2 and I^2, for decoupled user and beam forming in multi-user 60 GHz WLANs. We evaluated the spatial multiplexing gains as a function of performance factors such as receiver separation and AP's array size. We compared the performance of example S^2 and I^2 user selection policies and explored factors such as the number of RF chains and LOS vs. NLOS paths. We showed that if the AP has only two RF chains, low-complexity low-overhead S^2 policies can achieve up to 70% of the maximum achievable sum-rate. However, the performance gap between I^2 and S^2 policies increases as the number of RF chains and potential group size grows. We also showed that although NLOS users experience reduced signal strength, they can significantly benefit from multi-user aggregation. Lastly, while *joint* beam training and user selection via exhaustive search has prohibitive overhead, we experimentally compared it to the *decoupled* methodology.

9 ACKNOWLEDGEMENTS

This research was supported by Cisco, Intel, the Keck Foundation, and by NSF grants CNS-1642929, CNS-1514285, and CNS-1444056.

REFERENCES

[1] A. Alkhateeb and G. Leus and R. W. Heath. 2015. Limited Feedback Hybrid Precoding for Multi-User Millimeter Wave Systems. *IEEE Transactions on Wireless Communications* (2015).
[2] N. Anand, Jeongkeun Lee, Sung-Ju Lee, and E. W. Knightly. 2015. Mode and user selection for multi-user MIMO WLANs without CSI. In *IEEE Conference on Computer Communications (INFOCOM)*.
[3] Ehsan Aryafar, Narendra Anand, Theodoros Salonidis, and Edward W Knightly. 2010. Design and experimental evaluation of multi-user beamforming in wireless LANs. In *Proc. ACM MobiCom*.
[4] Oscar Bejarano, Edward W Knightly, and Minyoung Park. 2013. IEEE 802.11ac: from channelization to multi-user MIMO. *IEEE Communications Magazine* (2013).
[5] M. Esslaoui, F. Riera-Palou, and G. Femenias. 2012. A fair MU-MIMO scheme for IEEE 802.11ac. In *International Symposium on Wireless Communication Systems*.
[6] IEEE 802.11 Working Group. 2012. IEEE 802.11ad, Amendment 3: Enhancements for Very High Throughput in the 60 GHz Band. (2012).
[7] S. Hur, T. Kim, D. J. Love, J. V. Krogmeier, T. A. Thomas, and A. Ghosh. 2013. Millimeter Wave Beamforming for Wireless Backhaul and Access in Small Cell Networks. *IEEE Transactions on Communications* 61, 10 (2013), 4391–4403.
[8] J. Wang. 2009. Beam codebook based beamforming protocol for multi-Gbps millimeter-wave WPAN systems. *IEEE Journal on Selected Areas in Communications* (2009).
[9] C. Kim, T. Kim, and J. Y. Seol. 2013. Multi-beam transmission diversity with hybrid beamforming for MIMO-OFDM systems. In *2013 IEEE Globecom Workshops*.
[10] G. R. Maccartney, T. S. Rappaport, S. Sun, and S. Deng. 2015. Indoor Office Wideband Millimeter-Wave Propagation Measurements and Channel Models at 28 and 73 GHz for Ultra-Dense 5G Wireless Networks. *IEEE Access* (2015).
[11] N. Anand, E. Aryafar, E.W. Knightly. 2010. WARPlab: a flexible framework for rapid physical layer design,. In *Proceedings of the 2010 ACM workshop on Wireless of the students, by the students, for the students*.
[12] S. Naribole and E. Knightly. 2016. Scalable Multicast in Highly-Directional 60 GHz WLANs. In *2016 13th Annual IEEE International Conference on Sensing, Communication, and Networking (SECON)*.
[13] Mathew K. Samimi and Theodore S. Rappaport. 2015. Local Multipath Model Parameters for Generating 5G Millimeter-Wave 3GPP-like Channel Impulse Response. *CoRR* (2015).
[14] M. K. Samimi, S. Sun, and T. S. Rappaport. 2015. MIMO Channel Modeling and Capacity Analysis for 5G Millimeter-Wave Wireless Systems. *CoRR* (2015).
[15] A. M. Sayeed and V. Raghavan. 2007. Maximizing MIMO Capacity in Sparse Multipath With Reconfigurable Antenna Arrays. *IEEE Journal of Selected Topics in Signal Processing* 1, 1 (2007), 156–166.
[16] R. A. Stirling-Gallacher and M. S. Rahman. 2015. Multi-user MIMO strategies for a millimeter wave communication system using hybrid beam-forming. In *2015 IEEE International Conference on Communications (ICC)*.
[17] Shu Sun, George R. MacCartney Jr., and Theodore S. Rappaport. 2015. Millimeter-Wave Distance-Dependent Large-Scale Propagation Measurements and Path Loss Models for Outdoor and Indoor 5G Systems. *CoRR* (2015).
[18] S. Sur, I. Pefkianakis, X. Zhang, and K Kim. 2016. Practical MU-MIMO user selection on 802.11ac commodity networks. In *Proc. ACM MobiCom*.
[19] T. Tandai, H. Mori, and M. Takagi. 2009. Cross-layer-optimized user grouping strategy in downlink multiuser MIMO systems. In *IEEE 69th VTC*.
[20] X. Xie and X. Zhang. 2014. Scalable user selection for MU-MIMO networks. In *Proc. IEEE INFOCOM*.